Environmental Science Nano

Identification of Toxicity Effects of Cu2O Materials on C. elegans as a Function of Environmental Ionic Composition

Journal:	*Environmental Science: Nano*
Manuscript ID	EN-ART-06-2019-000686.R1
Article Type:	Paper

Environmental Significance Statement

In this manuscript, we have identified key components of material toxicity using the model animal, *Caenorhabditis elegans*. For these studies, we focused on materials composed of Cu_2O, which is a highly important photocatalyst for a variety of applications, including environmental remediation of toxic pollutants. Beyond simple composition, we have explored the effects of the sample environment on material toxicity. *C. elegans* was selected as it is well studied and can be easily monitored for a variety of toxicological effects of material exposure. Our results demonstrated that the Cu ion leaching from the Cu_2O materials is controlled as a function of the growth medium for the animal model; however, the toxicity of the particles is more than just simply from the release of Cu ions. This suggests that the particles themselves have a degree of toxicity that must be considering in their use in the environment. Such results demonstrate unique capabilities of this model system for understanding short- and long-term toxicological effects of potentially important materials for environmental applications.

Identification of Toxicity Effects of Cu_2O Materials on *C. elegans* as a Function of Environmental Ionic Composition

Catherine J. Munro,[a,c] Michelle A. Nguyen,[a,c] Christian Falgons,[a,b] Sana Chaudhry,[b] Mary Olagunjo,[a] Addys Bode,[b] Carla Bobé,[a,b] Manuel E. Portela,[a,b] Marc R. Knecht,[a,c] and Kevin M. Collins[b,c]

[a] Department of Chemistry

[b] Department of Biology

University of Miami, 1301 Memorial Drive, Coral Gables, Florida, 33146, USA.

[c] Equal contribution

* To whom correspondence should be addressed:

Email: kevin.collins@miami.edu, knecht@miami.edu

Electronic Supplementary Information (ESI) available: [movies of particle ingestion by worms]. See DOI: 10.1039/x0xx00000x

Abstract

Previous work has shown that spherical CuO nanomaterials show negative effects on cell and animal physiology. The biological effects of Cu_2O materials, which posess unique chemical features compared to CuO nanomaterials and can be synthesized in a similarly large variety of shapes and sizes, are comparatively less studied. Here, we synthesized truncated octahedral Cu_2O particles and characterized their structure, stability, and physiological effects in the nematode worm animal model, *Caenorhabditis elegans*. Cu_2O particles were found to be generally stable in aqueous media, although the particles did show signs of oxidation and leaching of Cu^{2+} within hours in worm growth media. The particles were found to be especially sensitive to inorganic phosphate (PO_4^{3-}) found in standard NGM nematode growth medium. Cu_2O particles were observed being taken up into the nematode pharynx and detected in the lumen of the gut. Toxicity experiments revealed that treatment with Cu_2O particles caused a significant reduction in animal size and lifespan. These toxic effects resembled treatment with Cu^{2+}, but measurements of Cu leaching, worm size, and long-term behavior experiments show the particles are more toxic than expected from Cu ion leaching alone. These results suggest worm ingestion of intact Cu_2O particles enhances their toxicity and behavior effects while particle exposure to environmental phosphate precipitates leached Cu^{2+} into biounavailable phosphate salts. Interestingly, the worms showed an acute avoidance of bacterial food with Cu_2O particles, suggesting that animals can detect chemical features of the particles and/or their breakdown products and actively avoid areas with them. These results will help to understand how specific, chemically-defined particles proposed for use in polluted soil and wastewater remediation affect animal toxicity and behaviors in their natural environment.

Introduction

The rational design of nanomaterials has yielded new technologies that have revolutionized diverse applications from biomedical diagnostics to catalysis. One specific example is the application of nanomaterials towards environmental remediation protocols, such as wastewater treatment or contaminant removal via catalytic processes.[1,2] In these approaches, oftentimes catalytic nanomaterials are dispersed into the environment to drive the catalytic degradation of known pollutants such as polychlorinated biphenyls, polybrominated diphenyl ethers, polychlorinated dibenzo-*p*-dioxins, and dibenzofurans;[3–7] however, the effects of nanomaterials released into the environment remain remarkably unknown where their own toxicity could rival or even surpass the toxicity of the original pollutant.

Metal oxide semiconductor photocatalysts are attractive materials for environmental remediation due to their reliance on renewable solar light as the main energy source to drive the reaction. In particular, Cu_2O has gained increasing interest as a material for the photocatalytic degradation of environmental pollutants due to its narrow band gap of 2.17 eV,[8] allowing it to exploit visible light absorption, a significantly greater portion of the solar spectrum. It has been demonstrated that Cu_2O has the ability to break down aromatic dyes that are known to be difficult to degrade.[6,9,10] This reaction occurs through the generation of reactive oxygen species at the metal oxide surface, leading to pollutant degradation.[11–13] Additionally, metal-containing nanoparticles can release toxic metal ions, such as Ag^+, Cu^{2+}, and Zn^{2+}, via dissolution in aquatic environments.[14,15] However, toxicity effects will undoubtedly vary depending on numerous parameters, such as metal oxidation state, particle size, surface properties, including the effects of any ligands that may be integrated

into the material during synthesis that could also be leached into the environment.[16] Metal-containing nanoparticles are likely to have dramatically different stability and catalytic properties in varying environments, for example at high or low ionic strength, at different pH, availability of salt-inducing counter ions, and in abiotic vs. biotic environments. Particle size and shape are anticipated to be highly important determinants of biocompatibility; smaller, hydrophilic particles are more likely to interact with or be taken up by organisms, leading to potential physiological effects.

In this study, *C. elegans* worms were used as a model organism to assess the short- and long-term toxicological and physiological impacts of newly synthesized truncated cuboctahedral Cu_2O microcrystals.[16] Previous work has shown that Ag, Au, Cu, and Si nanoparticles, but not Zn or Ce cause *C. elegans* feeding behaviour defects and premature lethality.[15,17–20] In general, the toxicity of metal oxide nanomaterials has been found to be less than release of an equivalent amount of metal ions alone.[21] Previous studies looking specifically at Cu-based nanoparticles were limited to small (30 nm) CuO particles with a spherical shape,[19] raising the question whether particle toxicity is a general feature of all Cu materials or specific to particular oxidation states, particle shapes, sizes, and/or surface chemistries. Here we show that truncated octahedral Cu_2O crystals, like CuO spherical nanoparticles, are toxic to the *C. elegans* animal model. This toxicity depended crucially on the ionic environment, with phosphate-containing growth medium causing enhanced particle degradation, reducing their bioavailability and physiological effects. In phosphate-deficient media, the Cu_2O particles were more stable and the particles were more toxic to worms than an equivalent amount of Cu^{2+} ion, suggesting the particle structure provides additional environmental stability and catalytic features. Because worms also avoid areas with Cu_2O particles, their toxicological

consequences are expected to be blunted further when encountered in the environment.

Materials and Methods

Chemicals. $CuSO_4 \cdot 5H_2O$, and 95% ethanol were obtained from BDH Chemicals, while glucose, cholesterol, $CaCl_2 \cdot 2H_2O$, potassium chloride, and sodium hydrogen phosphate were acquired from Alfa Aesar. Sodium hypochlorite was purchased from Clorox. Sodium hydroxide and sodium carbonate were from EMD Millipore. Bacto-tryptone was acquired from BD Biosciences. Sodium chloride and $MgSO_4 \cdot 7H_2O$ were obtained from Amresco. 5-Fluoro-2'-deoxyuridine (FUDR) was purchased from BioWorld. Finally, polyvinylpyrrolidone (PVP; MW ~29,000 g/mol), potassium phosphate dibasic, potassium phosphate monobasic, and sodium citrate were from Sigma Aldrich. All chemicals were used as received without further purification. Milli-Q water (18 MΩ·cm) was used for all experiments.

Synthesis of Cu_2O particles. Cu_2O truncated octahedra (1.1 μm) were fabricated according to synthetic protocols established by Sui *et al*.[22] Specifically, 1.5 mM of PVP was dissolved in 17 mL of an aqueous 38 mM $CuSO_4$ solution. Upon complete dissolution of the PVP, 1 mL of an aqueous solution containing both 0.37 M sodium citrate and 0.60 M sodium carbonate was added drop-wise with continuous stirring. This was followed by the addition of 1 mL of an aqueous 1.4 M glucose solution, which was again added drop-wise with continuous stirring. The reaction vessel was then placed in a 70 °C water bath for 2 h. Once complete, the dark red precipitate was filtered through a 0.1 μm polycarbonate membrane, thoroughly washed with water and ethanol, and dried under vacuum at 60 °C for at least 12 h.

Materials Characterization. Scanning electron microscopy (SEM) was performed using a FEI/Philips XL-30 Field Emission SEM. To prepare the sample, the Cu_2O materials were dispersed in ethanol via sonication, after which 10 µL of the sample was drop-casted onto an aluminium stub. Particle size distribution was determined by measuring ≥100 individual particles from multiple images of the synthesized material. UV-vis DRS analysis was completed on a Shimadzu Model UV-2600 system, scanning from 200–800 nm, using a 2 mm quartz cuvette as the sample holder. To analyse the materials after incubation with different worm growth media, the particles were dispersed in 95% ethanol (200 mg/mL) and diluted 50-fold in water (4 mg/mL). From this, 200 µL of the suspension was applied to each of four agar plates of each media type (see below) seeded with OP50 bacteria.[23] After incubation for 24 h at 25 °C, the particles were recovered from the plates by washing into 2 mL of water. The particles were then sedimented by centrifugation (170x g; 1 min), resuspended in 1 mL of sterile Milli-Q water, and recentrifuged. This resuspension procedure was repeated twice after which the aqueous supernatant was removed, leaving ~100 µL of water and particles. The particles were then diluted with 1 mL of 95% ethanol and re-centrifuged (1000x g; 1 min). Most of the supernatant was removed, and the remaining particles were resuspended in the residual ethanol (~100 µL) and applied to aluminium stubs and dried overnight at 25 °C for SEM analysis.

Cu^{2+} leaching experiments. Cu_2O particles (4 mg/mL; or ~3.5 mg/mL Cu equivalents) were resuspended in either distilled water, B-Broth only (per liter: 10 g Bacto-Tryptone, 5 g NaCl), or liquid Nematode Growth Medium (NGM), K Medium, or Low K Medium after inoculation with OP50 bacteria culture grown overnight in B-Broth (1:100 dilution of the OP50/B-Broth culture into each media type). Reactions (3

replicates for each incubation time) were run in microcentrifuge tubes with 1470 µL of water, the indicated medium, or B broth. 30 µL of a 200 mg/L Cu_2O particle suspension in ethanol was diluted, sealed, and vortexed for 5 s before it was left undisturbed for a given period (0 h, 1 h, 2 h, 8 h, 24 h, and 7 days). At the end of the reaction the time, the microcentrifuge tube was centrifuged at 8000 rpm for 1 min before 750 µL of the supernatant was extracted and diluted into 10% HNO_3 prior to being run for elemental analysis on Agilent 4200 MP-AES.

***Caenorhabditis elegans* worm culture and treatment with particles.** *C. elegans* Bristol N2 wild-type animals were maintained as hermaphrodites at 20 °C on nematode growth medium (NGM) agar plates seeded with *Escherichia coli* OP50 food grown in B broth as described.[23] NGM contained (per liter): 25 mM K_3PO_4 pH 6, 51.37 mM NaCl, 1 mM $CaCl_2$, 1 mM $MgSO_4$, 5 mg cholesterol, 2.5 g Bacto-Peptone, and 17 g Bacto-Agar. To test the effects of inorganic phosphate and ionic strength, K Medium was prepared, as described,[24] along with a derivative, Low K Medium, that has reduced ionic strength. K Medium is equivalent to NGM except 25 mM K_3PO_4 is replaced with 25 mM KCl. Low K Medium is K Medium with 10 mM KCl, 0 mM NaCl. Lawns of OP50 bacteria grown in NGM were at pH 6.0, while those in K Medium and Low K Medium agar plates were at pH 7.5.

Mixed stage, gravid adult worms grown on NGM were synchronized by bleaching and hatching of eggs in M9 buffer. Hatched L1 larvae were then dispensed onto the indicated media (NGM, K, and Low K) for ~48 h until they reached the L4 stage, after which they were treated with either vehicle control (2% ethanol), Cu_2O particles, or $CuSO_4$ solution. The concentrations indicated represent the total concentration of free copper ions (in mg/mL) available for release assuming 100% ionization. For

example, we assumed a molar weight of 143 g/mole for the Cu_2O particles of which ~89% of the mass is copper. As such, 4 mg/mL Cu_2O particles have ~3.5 mg/mL total ionizable copper, comparable to the ~3.2 mg/mL copper ion present in an equal volume of 50 mM $CuSO_4.5H_2O$ solution. Dried particles were resuspended in 95% ethanol at a concentration of 200 mg/mL and bath sonicated for 5 min. Particle suspensions in ethanol were found to be stable for weeks. Serial dilutions of nanoparticle stock solutions were performed in 95% ethanol. For behaviour assays, sonicated particles (or ethanol alone) were freshly diluted 50-fold with sterile Milli-Q water, vortexed, and 200 µL of the diluted suspension, vehicle, or $CuSO_4.5H_2O$ solution at the indicated concentrations was applied to each plate containing worms and bacteria. All behaviour assays were performed using age-matched adult hermaphrodites 24–40 h past the late L4 stage.

Survival. Long-term viability assays were performed as described.[33] Animals were synchronized through bleaching of gravid adults followed by hatching of eggs in M9 buffer. Approximately 30-40 arrested L1 larvae were deposited onto each of three 60 mm NGM, K Medium, or Low K Medium plates seeded with OP50 bacterial food and grown for ~48 h until they reached the late L4 stage. The bacterial lawn was then overlaid with 100 µL of 10 mg/mL FUDR, as described, to prevent overgrowth of the plate with worm progeny during the subsequent long-term incubations.[25–27] After the FUDR soaked into the plates, the L4 animals were overlaid with 200 µL of the freshly diluted aqueous particle suspensions, 2% ethanol vehicle control, or $CuSO_4$ at the indicated concentrations and incubated at 20 °C. Animals were tested for viability every 2-3 days by gentle prodding with a platinum worm pick.[28] An animal was considered dead if it showed no movement or pharyngeal pumping after mechanical stimulation.

Body length and worm recordings. Worms were recorded using a FLIR Grasshopper 3 USB3 camera (41C6NIR-C) with 2 by 2 binning through a Leica M165FC stereomicroscope using a PLAN APO 1.0x or 5.0x (0.5NA) objective, as described.[25] Ingestion and gut transport of particles was recorded at 30-60 frames per second. Average worm length was determined using FIJI software.[29] Briefly, a segmented line with ~10 points was drawn through the worm mid-body. Approximately 30 individuals per treatment condition were measured.

Particle avoidance. Plates with OP50 bacteria overlaid with diluted vehicle, particles, or $CuSO_4$ were prepared as above. A worm was considered on food if she was within one body length of the bacterial lawn, where ≥29 animals per treatment condition were measured.

Statistical procedures. Prism 7.0d (GraphPad) was used for statistical analyses of the biological studies. A p value of ≤0.05 was considered significant. Individual p values and statistical tests can be found in the figure legends. All tests were corrected to account for multiple comparisons.

Results and Discussion

We have previously shown that *C. elegans* worms can consume nanomaterials derivatized with novel fluorescent moieties, allowing for studies of their localization and optical properties *in vivo.*[30,31] In this contribution, we examine the uptake and toxicity of synthesized Cu_2O particles using established criteria of viability and health.[16] The Cu_2O composition was chosen for two specific reasons. First, it is becoming an important metal oxide photocatalyst with potential applications for environmental remediation, thus understanding its effects on biological systems is

important. Second, a variety of known synthetic methods are available to control the particle size and shape of Cu_2O.[8,22] This will allow for a holistic understanding of how composition, size, and shape contribute to the toxicological and physiological effects under different environmental conditions, specifically ionic strength and composition.

In the initial work described here, we focus specifically on the effects of ionic strength and composition using a single Cu_2O particle type, that of a truncated octahedra. The Cu_2O particles were generated by reducing a copper-citrate complex with glucose in the presence of PVP at 70 °C.[22] For this synthetic method, PVP acts as the stabilizing polymer to control the shape of the materials as the particle morphology is dictated by the amount of PVP. To achieve Cu_2O truncated octahedra, the copper-citrate complex was reduced by glucose with 1.5 mM PVP in the reaction mixture. Note that after synthesis, the particles were fully purified by washing with water followed by ethanol, thus any free polymer in the system is readily removed. SEM analysis of the prepared particles indicated predominantly truncated octahedra (Figure 1a). Size histograms showed a width of 1.1 ± 0.3 μm (Figure 1b). The UV-vis absorbance properties of the materials were evaluated using UV-vis DRS, and the absorption spectra of the Cu_2O particles are presented in Figure 1c. The materials exhibited strong absorption in the visible region, where the onset of visible light absorption started at ~650 nm. From this analysis, the band gap was determined using a Tauc plot,[32] which was found to be 2.09 eV (Figure 1d). Such a value is comparable to other Cu_2O materials previously reported.[6,8] Together, these results show the preparation of a uniform truncated octahedral particles with robust visible light absorption with a narrow band gap.

Having established the structural and optical properties of the particles, we next tested whether and how they affect the health and viability of the animal model, *Caenorhabditis elegans*, as they would be expected to interact with these particles introduced into the environment. Previous work indicates that that μg/mL and mg/mL levels of Cu^{2+} and ~30 nm spherical CuO nanoparticles, respectively, caused adverse physiological effects in laboratory and wild strains *C. elegans.*[19,24,33,34] In these prior studies, nanoparticle toxicity was greater than an equivalent amount of copper ion.[27] In contrast, a recent meta-analysis of nanoparticle toxicity showed that the particle form is typically less toxic to biological systems than similar levels of the dissolved metal ion.[21] To determine whether the larger (1.1 μm) Cu_2O particles prepared here cause toxic effects on *C. elegans*, we used the truncated octahedra as a model material for these studies.

We first tested the stability of the Cu_2O particles in culture media used for worms and the *E. coli* bacteria they consume. We observed no significant copper release from 4 mg/mL particles over seven days in purified Milli-Q water (Figure 2a). When the particles were incubated in NGM, K Medium lacking inorganic phosphate, or low ionic strength K Medium (Low K Medium) inoculated with OP50 bacteria, elemental analyses indicated a significant amount of copper was released within hours. To this end, for the K and Low K Media, the copper release concentration reached a value of ~0.5 mg/mL by 24 h; however, a lower value of 0.14 mg/mL copper was solubilized for the materials in phosphate-containing NGM. The copper release reached ~1 mg/mL after 7 days of incubation for K and Low K Media (Figure 2a), representing about one third of the total copper present in the particles in the starting dilution (~3.5 mg/mL). For the NGM Medium, notable copper release was achieved after 7 days, reaching a value of 0.61 mg/mL soluble copper, which is lower than that

observed for the phosphate free media. Copper release was significantly lower in worm growth media compared to B Broth used for growth of the OP50 bacterial food consumed by *C. elegans*. Incubation in B broth caused nearly complete copper release from the particles after seven days (Figure 2a). These elemental analyses indicate that the synthesized Cu_2O particles are generally stable in culture media used for the worm growth and behaviour experiments (which require ~1 to 25 days of analyses), although the particles do undergo time- and media-dependent release of soluble copper that might negatively affect *C. elegans*.

We observed that free, soluble copper levels were markedly lower after incubation in NGM compared to either K or Low K Media (Figure 2a), suggesting the Cu_2O particles were more stable on NGM. To our surprise, we noticed that on NGM plates, the standard growth media for *C. elegans*, the previously brick-red Cu_2O particles changed to a blue-green colour, consistent with oxidation of the particles (Figure 2b). Interestingly, the particles did not show this acute colour change when applied to growth media lacking added inorganic PO_4^{3-} (K or Low K Media) where the 25 mM K_3PO_4 was replaced with KCl (Figure 2b). The blue-green colour of the NGM-particles was consistent with particle oxidation and precipitation of $Cu_3(PO_4)_2$, and the blue green precipitate could be replicated by application of aqueous $CuSO_4$ solutions to NGM plates (data not shown). We examined the integrity of the particles in each growth medium, and we found that red K- and Low K-particles were stable for days while blue NGM-particles had become less visible (Figure 2c). Additionally, we used SEM to examine the morphology of the particles after incubation in each growth medium for 24 h. As expected for the particles in K and Low K growth Media, they generally retained the truncated octahedral shape and size of the original structures; however, their surfaces were more rough and a degree of pitting

observed (Figure 2d). This suggests that oxidation is happening in these media, leading to release of Cu ions to solution. Interestingly, the Cu_2O materials incubated in NGM had substantially less defined shapes, as compared to the original structures (Figure 2d), consistent with the loss of particle integrity observed by light microscopy on NGM but not K or Low K Media plates (Figure 2c). Such results are consistent with the observed leaching of Cu species to solution (Figure 2a). For all three media, release of Cu from the Cu_2O material is evident; however, for NGM our data suggest that the presence of PO_4^{3-} also leads to the precipitation of highly insoluble $Cu_3(PO_4)_2$. For the media without PO_4^{3-} (K and Low K), the Cu ions are released to solution as well, but do not precipitate. As such, higher Cu solution concentrations are anticipated from the K and Low K Media, consistent with the results of Figure 2a.

Worms were found to readily eat particles encountered with bacterial food on the surface of NGM and other growth media (Figure 3a and Supplemental Movie 1). Ingested NGM particles were then detectable inside the gut lumen (Figure 3b and Supplemental Movie 2). Previous experiments studying the size exclusion of particles in the worm pharynx suggested the 1.1 μm particles studied here are within the range of consumption and transport into the gut.[11] We have previously shown that fluorescent nanocarriers between 20 nm to 3 μm are also consumed by worms with food and deposited into gut.[30,31] These results indicate that the Cu_2O particles can be internalized by feeding into the worms as they consume similarly sized bacteria food.

Cu_2O particles were found to be deleterious to worm health and viability. On average, particle-treated worms were smaller and had a starved appearance compared to control worms (Figures 3c and 3d). As shown in Figure 4, we measured

the overall worm length after 24 h of particle (left) and Cu^{2+} treatments (right) in different growth media and found the treated worms failed to reach the same size as age-matched control animals treated with the ethanol vehicle (Figures 4a-c; compare to Figures 3c and 3d). Higher concentrations of particles were required to cause a significant effect on worm length in NGM compared to Cu^{2+} treatment (Figure 4a). This was not observed in K and Low K Media where particles and Cu^{2+} caused similar reductions in worm growth (compare Figures 4a to 4b-c). This is consistent with our observation that Cu_2O particles were more stable in phosphate-free media, which likely prolonged any adverse physiological and behavioural effects. Particles caused a similar reduction in worm length after 24 h as an equivalent level of total Cu in all media types except NGM (Figure 4), raising the question of whether Cu ion leaching from particles in K or Low K Media could be causative of the enhanced Cu_2O particle toxicity. As shown in Figure 4d, worms treated for 24 h with 4 mg/mL particles were considerably shorter than vehicle-treated animals (K Medium: 68.0 ± 2.6%; Low K Medium: 76.5 ± 2.4). Because ~0.5-1 mg/mL Cu is released from 4 mg/mL particles after 24 h (Figure 2a), the detrimental effect of Cu_2O particles on worm length was stronger than treatment with 0.5 or 1.0 mg/mL Cu^{2+} alone (K Medium: 84.4±2.8%; Low K Medium: 90.3±3.1%) (Figures 4c and 4d, compare grey boxes). As a result, we conclude that levels of Cu^{2+} leached from Cu_2O particles into the growth media are insufficient to explain the observed reduction of worm length, although oxidation and release of other toxic Cu species, particularly after concentration in the lumen of the worm intestine, cannot be excluded.

We next tested the consequences of long-term incubation with the Cu_2O particles using survival assays. Median lifespan of animals grown and treated in NGM (Figure 5a), the phosphate-containing growth medium in which we see the lowest levels of

soluble Cu released, was only affected at the highest doses of particles tested, 4 mg/mL (Figures 5a and 5g). In contrast, animals grown in K and Low K Media showed adverse effects at 1 mg/mL (Figure 5b) and 0.125 mg/mL (Figure 5c), respectively. As summarized in Figure 5g, animals treated with Cu_2O particles showed a significant reduction in lifespan (median 10 days after reaching adulthood) compared to untreated control animals (17 days). This reduction in lifespan depended critically upon the growth media with worms grown on K or Low K Media showing enhanced sensitivity to Cu_2O particle exposure (Figure 5g).

To determine whether Cu leaching could be causative of the observed particle toxicity, we compared the survival of animals treated with Cu_2O particles to those treated with soluble Cu^{2+}. Median (50%) survival of worms treated with 4 mg/mL Cu_2O particles, which we have previously shown release ~1 mg/mL soluble Cu after 7 days on all three media types, was ~10 days while survival of worms treated with 1 mg/mL free Cu^{2+} was 14 days. As such, it took 4 mg/mL Cu^{2+} to causes a quantitatively similar decrease in worm survival as seen for 4 mg/mL Cu_2O particles (Figure 5h). Because Cu leaching from 4 mg/mL particles is ~1 mg/mL by this timepoint (Figure 2a), we interpret this result as indicating Cu_2O particles are more toxic than expected if Cu^{2+} leaching into the surrounding growth media was their primary mode of toxicity (Figure 5i). Because Cu oxidation and leaching from particles occurs on the order of days in K and Low K Media, while Cu^{2+} exposure was initiated on day 0, these results are likely underestimating the toxicity of Cu_2O particles relative to Cu^{2+}. Thus, Cu_2O particle toxicity is distinct from Cu^{2+} leaching, although leaching of other toxic forms of Cu and/or their combined toxic effects with the particulate form could be synergistic. For example, because the Cu_2O particles are similar in size to the worm's bacterial food, accumulation of the particles into the

gut during feeding may lead to an increase in particle concentration relative to the external environment.[35] Mechanical disruption of the particles is also expected as the food passes into the pharyngeal grinder which might accelerate particle dissolution in the gut lumen, enhancing toxicity.[36] Our results further suggest that inorganic phosphate present in NGM reduces particle and Cu^{2+} toxicity by decreasing the bioavailability of leached Cu^{2+} by the precipitation of insoluble phosphate salts.

These experiments indicate that Cu_2O particles have significant detrimental consequences on worm viability when the animals were given no alternate food source or opportunity to escape. Worms typically spend most of their time in the lawns of *E. coli* bacterial food, showing only infrequent trips away from the lawn (Figure 6a). However, we found worms avoided food containing Cu_2O particles after 24 h (Figure 6b). We measured the proportion of animals found off food treated with the different levels of particles (Figure 6c). Worms began avoiding lawns of bacteria with particles even at low concentrations (0.25 mg/mL), with complete avoidance observed at the highest particle levels, 4 mg/mL. Particle avoidance at 24 h was largely recapitulated by Cu^{2+} ion, with ~50% of worms showing avoidance at 2 mg/mL Cu^{2+} applied, independent of media type (Figure 6d). Levels of Cu ion leached from 4 mg/mL particles after 24 h reaches only ~0.5 mg/mL (Figure 2a), a level of Cu^{2+} which by itself only causes modest avoidance effects (Figure 6d, filled grey box). Together, these results suggest that Cu^{2+} leaching is not responsible for worm avoidance of the Cu_2O particles.

These results show that Cu_2O particles are generally aversive to worms, with worms detecting and avoiding food areas containing particles. Why do worms exposed to Cu_2O particles die? Because of the phenotypic similarities between Cu_2O

and Cu^{2+} treatment, our data are consistent with one mode of Cu_2O particle toxicity occurs via particle oxidation and leaching of toxic Cu^{2+} ions. Contamination of bacterial food could affect *C. elegans* viability both acutely and after long-term exposure. Cu^{2+} is aversive to *C. elegans*, typically activating nociceptive sensory neurons and leading to the avoidance behaviour we observe.[37] The shortened lifespan and reduction of animal growth could be a direct result of starvation. Metals like Cu^{2+} are also taken up into *C. elegans* and cells via the transporters expressed in the gut and other tissues, and loss of these transporters reduces metal uptake and acute toxicity.[38] Metals are detoxified by ABC transporters that efflux accumulated metal ions, and loss of these transporters enhances metal toxicity by preventing their removal.[39] Once inside cells, heavy metals like Cu^{2+} have long-established toxic effects, interacting with thiol containing molecules in cells and increasing reactive oxygen species.[40,41] Our results are consistent with previous results with CuO nanoparticles which show enhanced toxicity in the particle form,[19] and toxicity results for both particle types may relate to their size and/or sensitivity to oxidation. Phosphate-containing media led to the formation of insoluble $Cu_3(PO_4)_2$ salts and a reduction in toxicity. As such, the Cu_2O particles in phosphate-free media have the potential to deliver more of the toxic Cu^{2+} form through particle oxidation. In the absence of PO_4^{3-}, these copper ions remain in solution, leading to animal exposure. We propose that mechanical disruption of ingested particles during passage through the pharyngeal grinder will increase their surface area, facilitating oxidation and copper ion dissolution. Such concentrated uptake should elevate Cu^{2+} levels in the gut lumen to levels much higher than equimolar concentrations of $CuSO_4$ in the medium. It might also trigger pharyngeal spitting or learned sensory avoidance behaviours[37,42,43]. Alternatively, nanosized materials may have additional mechanical

consequences on *C. elegans* feeding and other behaviours separate from the catalytic properties of the materials.[44] These could contribute to our observation that worms avoid Cu_2O particles more than Cu^{2+} alone. Future work will test whether particles of different size or shape have altered stability and toxicity in different growth conditions and ionic environments. Use of defined *C. elegans* mutants with predicted defects in Cu^{2+} avoidance behaviour or alterations in metal ion uptake should reveal whether the reduced viability we observe is caused by starvation or metal uptake. Additional measurements of metal toxicity, including morphological defects of neuron development, could help explain how Cu_2O nanomaterials affect animal viability.[19,20] Such results illustrate that while these materials demonstrate promise for environmental remediation applications, they might degrade to soluble toxic or insoluble non-toxic materials. This indicates that while great effort should be made to fully examine catalytic materials for clean-up of toxic sites, the long-term effects of release of nanomaterials must also be examined to determine their inherent toxicity and environmental effects.

Conclusions

Here we document the synthesis and functional characterization of truncated octahedral Cu_2O crystals and their effects on an animal model. We show using the nematode worm, *Caenorhabditis elegans*, that Cu_2O particles have both acute and long-term toxic effects, reducing animal feeding and viability. Indeed, the worms actively choose to avoid areas that are contaminated with particles. Cu_2O particle toxicity is enhanced at reduced ionic strength and reduced in the presence of inorganic phosphate, suggesting environmental factors affect particle stability and

catalytic perdurance. These results show that Cu_2O particles may provide a safe alternative to treatment of environmental pollutants if their oxidation and release of toxic Cu^{2+} ions can be eliminated.

Conflicts of interest

There are no conflicts to declare.

Acknowledgements

C.B., C.F., and M.E.P. acknowledges support from an NSF funded REU program (CHE-1560103). K.M.C. acknowledges support from grants from the NSF (IOS-1844657) and the NIH (R01-NS086932). We thank the University of Miami and the undergraduate students of the Biology & Chemistry Integrated labs for additional research support during the development of this project.

Notes and references

1 Z. Wu, G. Zhao, Y. Zhang, J. Liu, Y. Zhang and H. Shi, A solar-driven photocatalytic fuel cell with dual photoelectrode for simultaneous wastewater treatment and hydrogen production, *Journal of Materials Chemistry A*, 2015, **3**, 3416–3424.

2 C. Su, X. Duan, J. Miao, Y. Zhong, W. Zhou, S. Wang and Z. Shao, Mixed Conducting Perovskite Materials as Superior Catalysts for Fast Aqueous-Phase Advanced Oxidation: A Mechanistic Study, *ACS Catal.*, 2017, **7**, 388–397.

3 M. A. Nguyen, E. M. Zahran, A. S. Wilbon, A. V. Besmer, V. J. Cendan, W. A. Ranson, R. L. Lawrence, J. L. Cohn, L. G. Bachas and M. R. Knecht, Converting Light Energy to Chemical Energy: A New Catalytic Approach for Sustainable Environmental Remediation, *ACS Omega*, 2016, **1**, 41–51.

4 R. Zhao, D. Jin, H. Yang, S. Lu, P. M. Potter, C. Du, Y. Peng, X. Li and J. Yan, Low-Temperature Catalytic Decomposition of 130 Tetra- to Octa-PCDD/Fs Congeners over CuOX and MnOX Modified V2O5/TiO2–CNTs with the Assistance of O3, *Environ. Sci. Technol.*, 2016, **50**, 11424–11432.

5 E. B. Miller, E. M. Zahran, M. R. Knecht and L. G. Bachas, Metal oxide semiconductor nanomaterial for reductive debromination: Visible light degradation of polybrominated diphenyl ethers by Cu2O@Pd nanostructures, *Applied Catalysis B: Environmental*, 2017, **213**, 147–154.

6 M. A. Nguyen, N. M. Bedford, Y. Ren, E. M. Zahran, R. C. Goodin, F. F. Chagani, L. G. Bachas and M. R. Knecht, Direct Synthetic Control over the Size, Composition, and Photocatalytic Activity of Octahedral Copper Oxide Materials: Correlation Between Surface Structure and Catalytic Functionality, *ACS Appl. Mater. Interfaces*, 2015, **7**, 13238–13250.

7 E. M. Zahran, N. M. Bedford, M. A. Nguyen, Y.-J. Chang, B. S. Guiton, R. R. Naik, L. G. Bachas and M. R. Knecht, Light-Activated Tandem Catalysis Driven by Multicomponent Nanomaterials, *J. Am. Chem. Soc.*, 2014, **136**, 32–35.

8 J.-Y. Ho and M. H. Huang, Synthesis of Submicrometer-Sized Cu2O Crystals with Morphological Evolution from Cubic to Hexapod Structures and Their Comparative Photocatalytic Activity, *J. Phys. Chem. C*, 2009, **113**, 14159–14164.

9 C. Xu, L. Cao, G. Su, W. Liu, H. Liu, Y. Yu and X. Qu, Preparation of ZnO/Cu2O compound photocatalyst and application in treating organic dyes, *Journal of Hazardous Materials*, 2010, **176**, 807–813.

10 S.-K. Li, F.-Z. Huang, Y. Wang, Y.-H. Shen, L.-G. Qiu, A.-J. Xie and S.-J. Xu, Magnetic Fe 3 O 4 @C@Cu 2 O composites with bean-like core/shell nanostructures : Synthesis, properties and application in recyclable photocatalytic degradation of dye pollutants, *Journal of Materials Chemistry*, 2011, **21**, 7459–7466.

11 S. Padmaja and S. A. Madison, Hydroxyl radical-induced oxidation of azo dyes: a pulse radiolysis study, *J. Phys. Org. Chem.*, 1999, **12**, 221–226.

12 J. Cao, B. Luo, H. Lin, B. Xu and S. Chen, Visible light photocatalytic activity enhancement and mechanism of AgBr/Ag3PO4 hybrids for degradation of methyl orange, *Journal of Hazardous Materials*, 2012, **217–218**, 107–115.

13 L. Yu, J. Xi, M.-D. Li, H. Tat Chan, T. Su, D. Lee Phillips and W. Kin Chan, The degradation mechanism of methyl orange under photo-catalysis of TiO 2, *Physical Chemistry Chemical Physics*, 2012, **14**, 3589–3595.

14 N. M. Franklin, N. J. Rogers, S. C. Apte, G. E. Batley, G. E. Gadd and P. S. Casey, Comparative Toxicity of Nanoparticulate ZnO, Bulk ZnO, and ZnCl2 to a Freshwater Microalga (Pseudokirchneriella subcapitata): The Importance of Particle Solubility, *Environ. Sci. Technol.*, 2007, **41**, 8484–8490.

15 X. Yang, A. P. Gondikas, S. M. Marinakos, M. Auffan, J. Liu, H. Hsu-Kim and J. N. Meyer, Mechanism of Silver Nanoparticle Toxicity Is Dependent on Dissolved Silver and Surface Coating in Caenorhabditis elegans, *Environ. Sci. Technol.*, 2012, **46**, 1119–1127.

16 A. von Mikecz, Lifetime eco-nanotoxicology in an adult organism: where and when is the invertebrate C. elegans vulnerable?, *Environ. Sci.: Nano*, 2018, **5**, 616–622.

17 A. Albanese and W. C. W. Chan, Effect of Gold Nanoparticle Aggregation on Cell Uptake and Toxicity, *ACS Nano*, 2011, **5**, 5478–5489.

18 O. V. Tsyusko, J. M. Unrine, D. Spurgeon, E. Blalock, D. Starnes, M. Tseng, G. Joice and P. M. Bertsch, Toxicogenomic Responses of the Model Organism Caenorhabditis elegans to Gold Nanoparticles, *Environ. Sci. Technol.*, 2012, **46**, 4115–4124.
19 M. J. Mashock, T. Zanon, A. D. Kappell, L. N. Petrella, E. C. Andersen and K. R. Hristova, Copper Oxide Nanoparticles Impact Several Toxicological Endpoints and Cause Neurodegeneration in Caenorhabditis elegans, *PLOS ONE*, 2016, **11**, e0167613.
20 A. Piechulek and A. von Mikecz, Life span-resolved nanotoxicology enables identification of age-associated neuromuscular vulnerabilities in the nematode Caenorhabditis elegans., *Environ Pollut*, 2018, **233**, 1095–1103.
21 D. A. Notter, D. M. Mitrano and B. Nowack, Are nanosized or dissolved metals more toxic in the environment? A meta-analysis, *Environ. Toxicol. Chem.*, 2014, **33**, 2733–2739.
22 Y. Sui, W. Fu, H. Yang, Y. Zeng, Y. Zhang, Q. Zhao, Y. Li, X. Zhou, Y. Leng, M. Li and G. Zou, Low Temperature Synthesis of Cu2O Crystals: Shape Evolution and Growth Mechanism, *Crystal Growth & Design*, 2010, **10**, 99–108.
23 S. Brenner, The genetics of Caenorhabditis elegans, *Genetics*, 1974, **77**, 71–94.
24 P. L. Williams and D. B. Dusenbery, Using the nematode Caenorhabditis elegans to predict mammalian acute lethality to metallic salts, *Toxicol Ind Health*, 1988, **4**, 469–478.
25 K. M. Collins, A. Bode, R. W. Fernandez, J. E. Tanis, J. C. Brewer, M. S. Creamer and M. R. Koelle, Activity of the C. elegans egg-laying behavior circuit is controlled by competing activation and feedback inhibition, *Elife*, 2016, **5**, e21126.
26 B. Ravi, J. Garcia and K. M. Collins, Homeostatic feedback modulates the development of two-state patterned activity in a model serotonin motor circuit in Caenorhabditis elegans, *J. Neurosci.*, 2018, **38**, 6283–6298.
27 D. H. Mitchell, J. W. Stiles, J. Santelli and D. R. Sanadi, Synchronous growth and aging of Caenorhabditis elegans in the presence of fluorodeoxyuridine, *J Gerontol*, 1979, **34**, 28–36.
28 D. S. Wilkinson, R. C. Taylor and A. Dillin, Analysis of aging in Caenorhabditis elegans, *Methods Cell Biol.*, 2012, **107**, 353–381.
29 J. Schindelin, I. Arganda-Carreras, E. Frise, V. Kaynig, M. Longair, T. Pietzsch, S. Preibisch, C. Rueden, S. Saalfeld, B. Schmid, J.-Y. Tinevez, D. J. White, V. Hartenstein, K. Eliceiri, P. Tomancak and A. Cardona, Fiji: an open-source platform for biological-image analysis, *Nature Methods*, 2012, **9**, 676–682.
30 S. Tang, Y. Zhang, P. Dhakal, L. Ravelo, C. L. Anderson, K. M. Collins and F. M. Raymo, Photochemical Barcodes, *J. Am. Chem. Soc.*, 2018, **140**, 4485–4488.
31 E. R. Thapaliya, Y. Zhang, P. Dhakal, A. S. Brown, J. N. Wilson, K. M. Collins and F. M. Raymo, Bioimaging with Macromolecular Probes Incorporating Multiple BODIPY Fluorophores, *Bioconjug. Chem.*, 2017, **28**, 1519–1528.
32 C.-H. Kuo, C.-H. Chen and M. H. Huang, Seed-Mediated Synthesis of Monodispersed Cu2O Nanocubes with Five Different Size Ranges from 40 to 420 nm, *Advanced Functional Materials*, 2007, **17**, 3773–3780.
33 S. Moyson, K. Vissenberg, E. Fransen, R. Blust and S. J. Husson, Mixture effects of copper, cadmium, and zinc on mortality and behavior of Caenorhabditis elegans, *Environ. Toxicol. Chem.*, 2018, **37**, 145–159.
34 H. Fueser, N. Majdi, A. Haegerbaeumer, C. Pilger, H. Hachmeister, P. Greife, T. Huser and W. Traunspurger, Analyzing life-history traits and lipid storage using CARS microscopy for assessing effects of copper on the fitness of Caenorhabditis elegans, *Ecotoxicol. Environ. Saf.*, 2018, **156**, 255–262.
35 H. Schulenburg and M.-A. Félix, The Natural Biotic Environment of Caenorhabditis elegans, *Genetics*, 2017, **206**, 55–86.
36 Live and dead GFP-tagged bacteria showed indistinguishable fluorescence in Caenorhabditis elegans gut. - PubMed - NCBI, https://www.ncbi.nlm.nih.gov/pubmed/23812817, (accessed 14 November 2019).
37 M. A. Hilliard, A. J. Apicella, R. Kerr, H. Suzuki, P. Bazzicalupo and W. R. Schafer, In vivo imaging of C. elegans ASH neurons: cellular response and adaptation to chemical repellents, *EMBO J.*, 2005, **24**, 63–72.

38 C. Au, A. Benedetto, J. Anderson, A. Labrousse, K. Erikson, J. J. Ewbank and M. Aschner, SMF-1, SMF-2 and SMF-3 DMT1 Orthologues Regulate and Are Regulated Differentially by Manganese Levels in C. elegans, *PLOS ONE*, 2009, **4**, e7792.

39 M. S. Schwartz, J. L. Benci, D. S. Selote, A. K. Sharma, A. G. Y. Chen, H. Dang, H. Fares and O. K. Vatamaniuk, Detoxification of multiple heavy metals by a half-molecule ABC transporter, HMT-1, and coelomocytes of Caenorhabditis elegans, *PLoS ONE*, 2010, **5**, e9564.

40 L. M. Gaetke, H. S. Chow-Johnson and C. K. Chow, Copper: Toxicological relevance and mechanisms, *Arch Toxicol*, 2014, **88**, 1929–1938.

41 S. Puig and D. J. Thiele, Molecular mechanisms of copper uptake and distribution, *Curr Opin Chem Biol*, 2002, **6**, 171–180.

42 N. Bhatla, R. Droste, S. R. Sando, A. Huang and H. R. Horvitz, Distinct Neural Circuits Control Rhythm Inhibition and Spitting by the Myogenic Pharynx of C. elegans, *Current Biology*, 2015, **25**, 2075–2089.

43 E. Pradel, Y. Zhang, N. Pujol, T. Matsuyama, C. I. Bargmann and J. J. Ewbank, Detection and avoidance of a natural product from the pathogenic bacterium Serratia marcescens by Caenorhabditis elegans, *PNAS*, 2007, **104**, 2295–2300.

44 C. Fang-Yen, L. Avery and A. D. T. Samuel, Two size-selective mechanisms specifically trap bacteria-sized food particles in Caenorhabditis elegans, *Proc. Natl. Acad. Sci. U.S.A.*, 2009, **106**, 20093–20096.

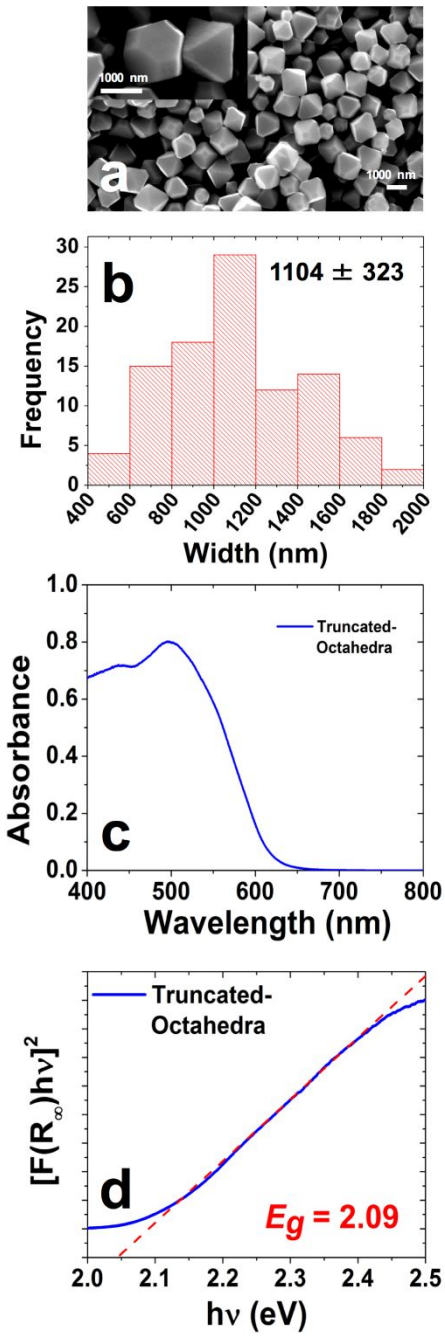

Figure 1: Comprehensive characterization of truncated octahedra Cu_2O micro crystals (a) SEM images of the Cu_2O particles. (b) Histogram of the particle size distribution. Particle sizes represent the average over at least 100 particles ± one standard deviation. (c) UV-vis absorption spectra of the truncated octahedra Cu_2O material. (d) Tauc plot of the Cu_2O particles studied.

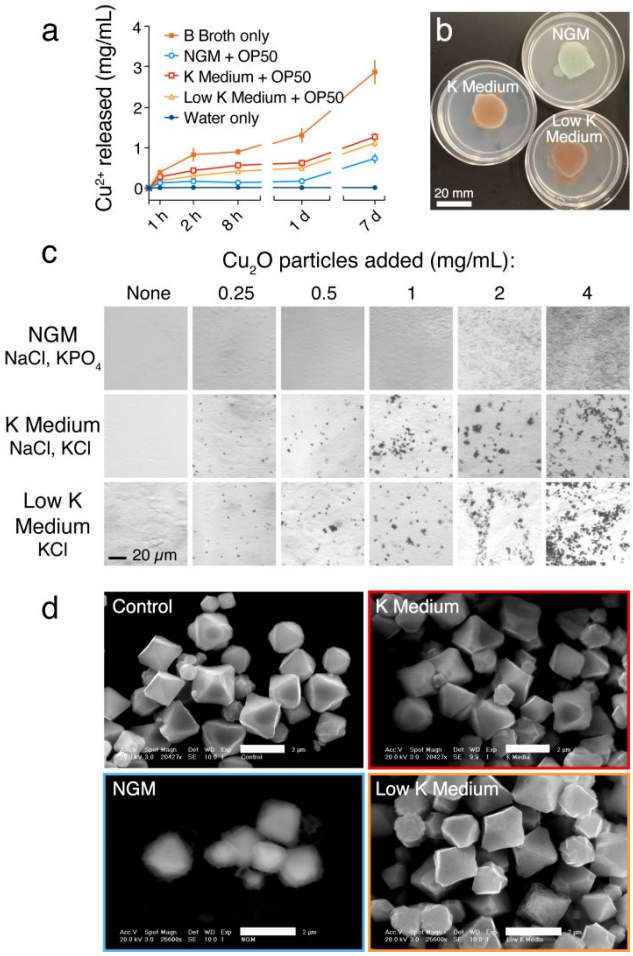

Figure 2: Chemical stability of Cu_2O particles. (a) Chemical determination of copper ion release from 4 mg/mL Cu_2O materials incubated in uninoculated B Broth (filled red squares), NGM (blue open circles), K Medium (red open squares), Low K Medium (open orange triangles) inoculated with OP50 bacteria, or distilled water alone (filled blue circles), at 25 °C for 7 days. (b) Particles (4 mg/mL) were applied to phosphate-containing NGM (top right), phosphate-free K Medium (left), or Low K Medium (lower right) agar plates seeded with OP50 bacteria. Particles in NGM became blue-green after incubation at 25 °C for 24 h, while particles in K or Low K Medium remained brick red. Scale bar, 20 mm. (c) Brightfield micrographs of increasing concentrations of Cu_2O particles applied to each media type after incubation at 25 °C for 24 h. Scale bar, 20 μm. (d) SEM analysis of particles before (Control) and after incubation at 25 °C for 24 h in NGM (blue), K Medium (red), or Low K Medium (orange). Bar, 2 μm.

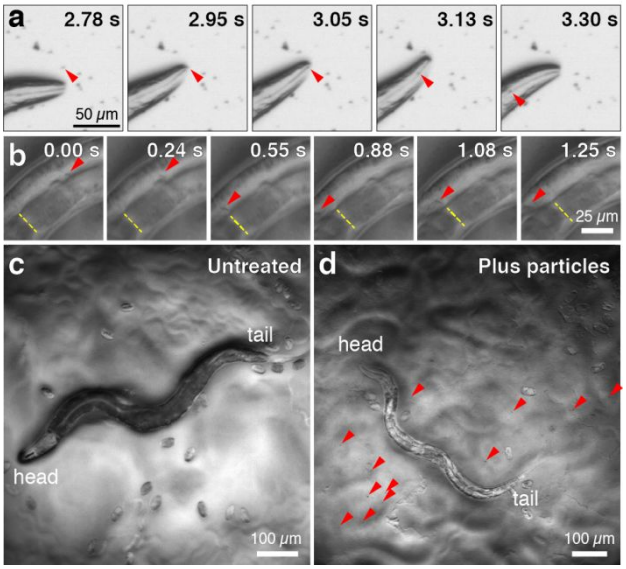

Figure 3. *C. elegans* worms consume Cu_2O particles. Animals were incubated at 20 °C for 24 h with 2% ethanol vehicle alone or 4 mg/mL Cu_2O particles on top of lawns of OP50 bacterial food in NGM. Red arrowheads indicate visible particles. Still images from video recordings show particle uptake into the pharynx (a) and movement within the gut (b). Yellow dotted line provides a worm landmark of the gut to highlight relative movement of the ingested particle aggregate. See also Supplemental Movies 1 and 2. Micrographs of worms after incubation for 24 h with (c) 2% ethanol vehicle alone or (d) with 4 mg/mL Cu_2O particles on top of lawns of OP50 bacterial food. Arrowheads indicate particles visible on the surface of the food; bar, 100 μm.

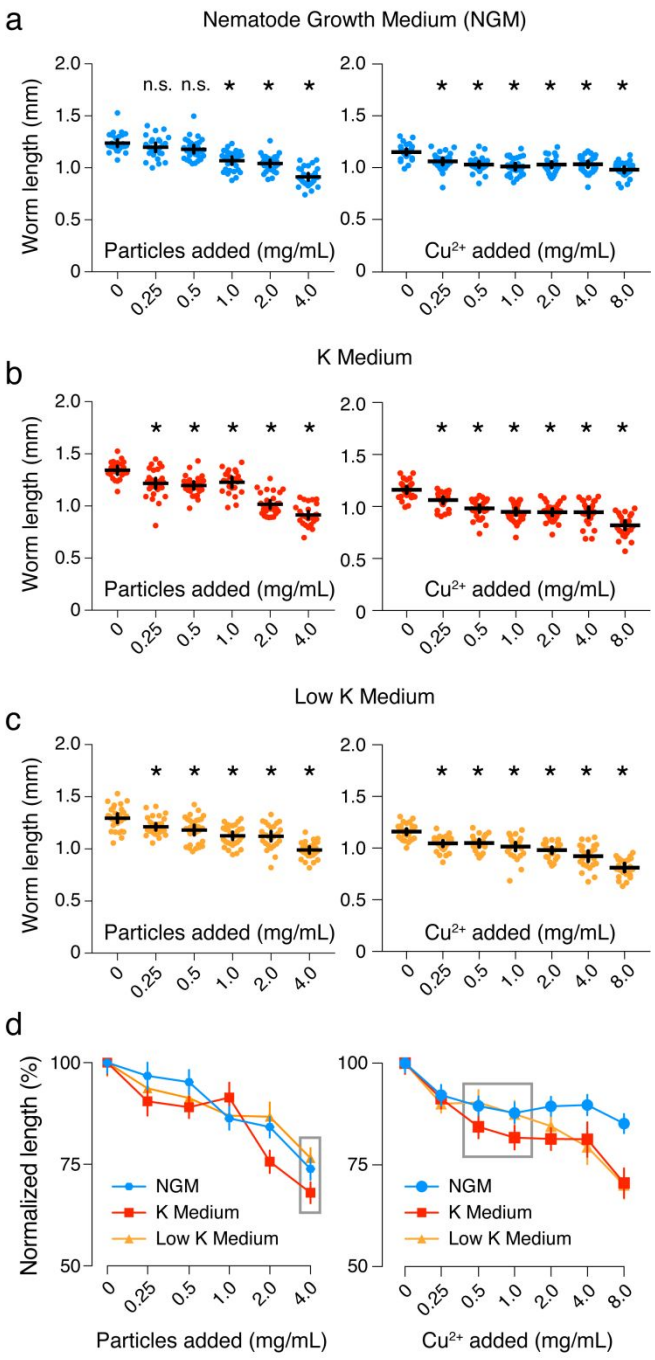

Figure 4. Cu_2O particle treatment reduces worm length. Scatterplots showing length of worms grown in NGM (a, blue) K Medium (b, red) or Low K Medium (c, orange) after incubation with the indicated concentrations of particles for 24 h. Individual points indicate the length of a single worm (n ≥22 animals per treatment). Lines/Symbols indicate average length ±95% confidence intervals. Asterisks indicate significant differences in length compared to vehicle treatment alone within a media and treatment group ($p < 0.05$, one-way ANOVA with Bonferroni correction for multiple comparisons); n.s. indicates means not significant ($p > 0.05$). (d) Normalized changes in worm length by added particles in

NGM (blue hexagons), K Medium (red squares), and Low K Medium (orange triangles). Mean length without particles (vehicle only) was set to 100%. Error bars indicate 95% confidence intervals. Grey boxes indicate changes in normalized worm length at comparable levels of soluble Cu released by particles into K and Low K Medium after 24 hours, as previously determined in Figure 2a.

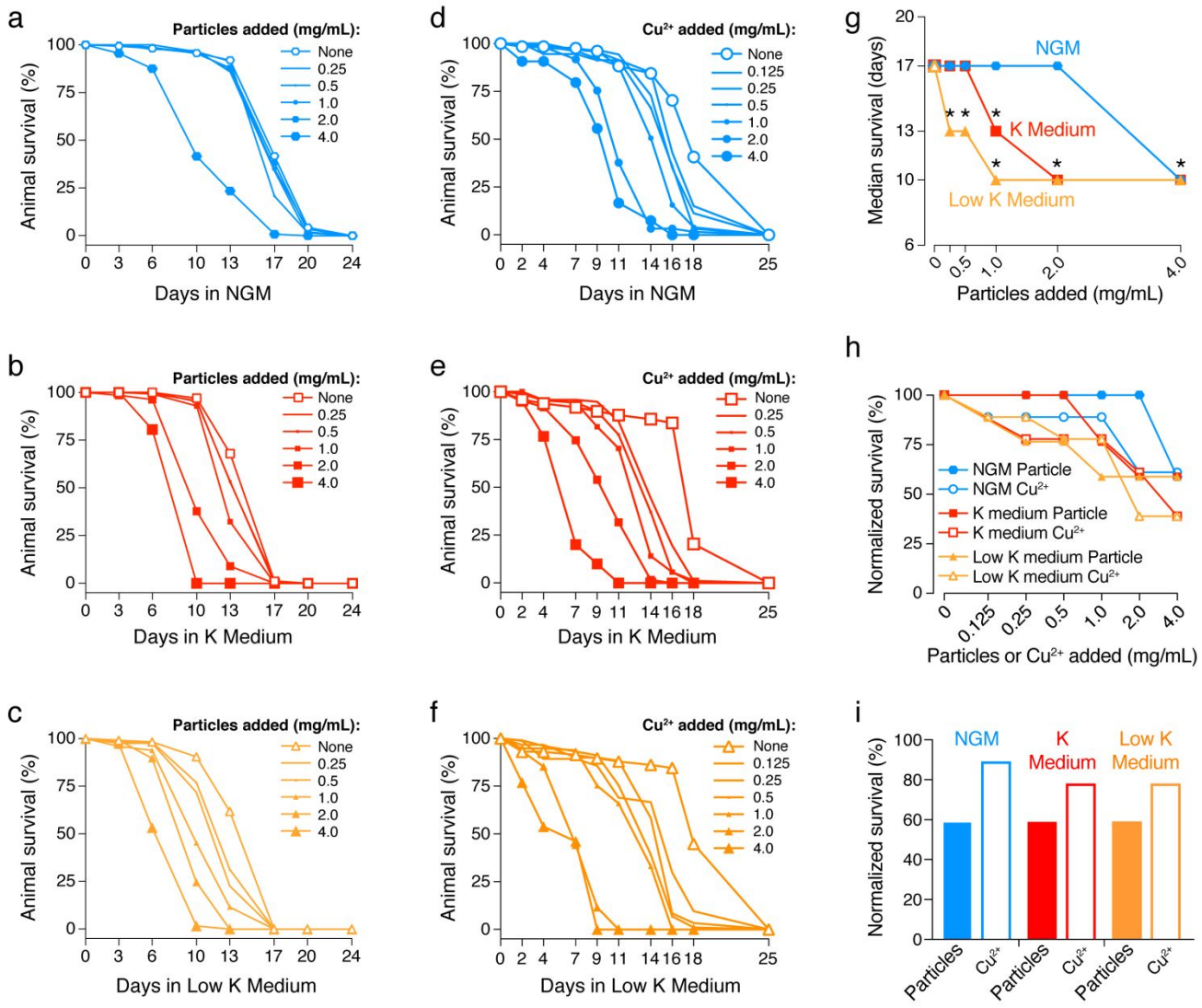

Figure 5. Cu_2O particles have enhanced long-term toxicity compared to Cu^{2+} ions alone. Adult *C. elegans* worms grown in (a,d) NGM (blue hexagons or circles), (b,e) K Medium (red squares), or (c,f) Low K Medium (yellow triangles) with OP50 bacterial food overlaid with the indicated concentrations of Cu_2O particles (a, b, c) or $CuSO_4$ measured in mg/mL Cu added (d, e, f) (filled symbols) or a vehicle control (open symbols). Worm viability of each treatment group was examined every 2-4 days for ~4 weeks. Asterisks indicate significant differences in median survival times (g) compared to vehicle-treated controls from the same growth media type (p<0.0005; Mantel-Cox Log-rank test with Bonferroni correction). (h) Median survival normalized as a percent of vehicle-treated animals (set to 100%) after treatment with Cu_2O particles or Cu^{2+} ion on each media type. (i) Normalized median survival of animals treated with 4 mg/mL particles or 1 mg/mL Cu^{2+}, an equivalent level of Cu leached from 4 mg/mL particles after ~7 days.

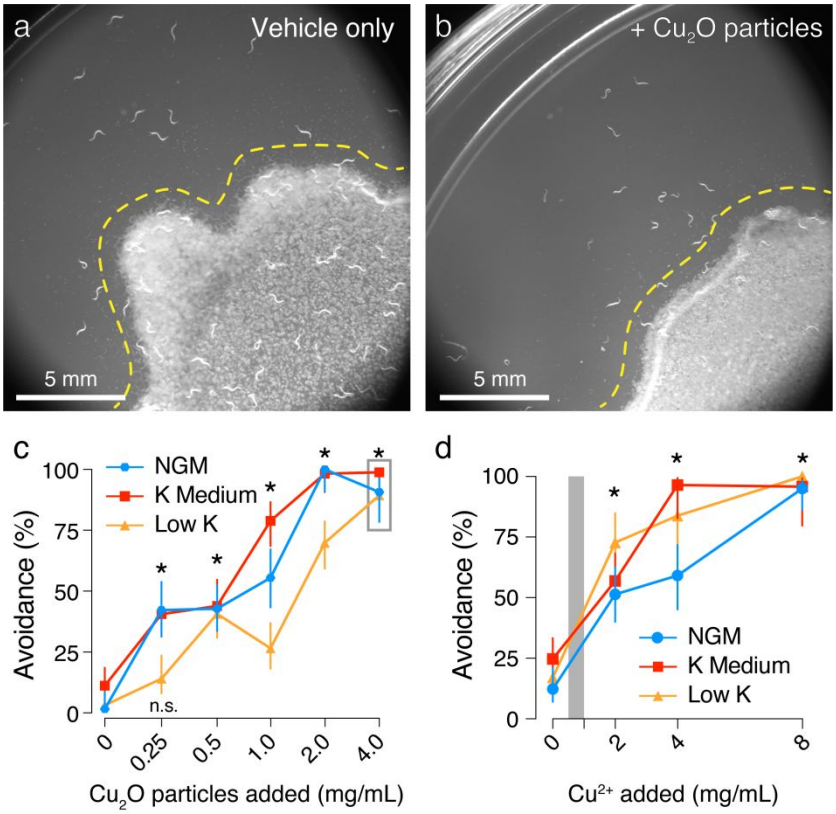

Figure 6. Worms avoid Cu_2O particles. Darkfield micrographs of worms on lawns of bacterial food treated with either (a) vehicle control or (b) 2 mg/mL Cu_2O particles; worms are indicated in white. Percent of animals found within one worm body length of the food (yellow dotted line) after treatment with particles (c) or Cu^{2+} alone (d) were measured in either NGM (blue hexagons or circles), K Medium (red squares), or Low K Medium (orange triangles). 4 mg/mL Cu_2O particles (c, open grey box) leach ~0.5-1 mg/mL Cu ion after 24 h (Figure 2a), a comparable level indicated by the filled grey box in (d). Error bars indicate the mean proportion ± 95% confidence intervals (n≥39 animals). Asterisks indicate significant differences in the proportion of animals found on 0.25 mg/mL (and greater) particle-treated lawns or 2 mg/mL Cu^{2+} treated lawns compared to the vehicle-only control of the same media type ($p < 0.0015$), except for Low K Medium which was not found to be significantly different until 0.5 mg/mL; n.s. indicates $p > 0.05$ (Fisher Exact test with Bonferroni correction).

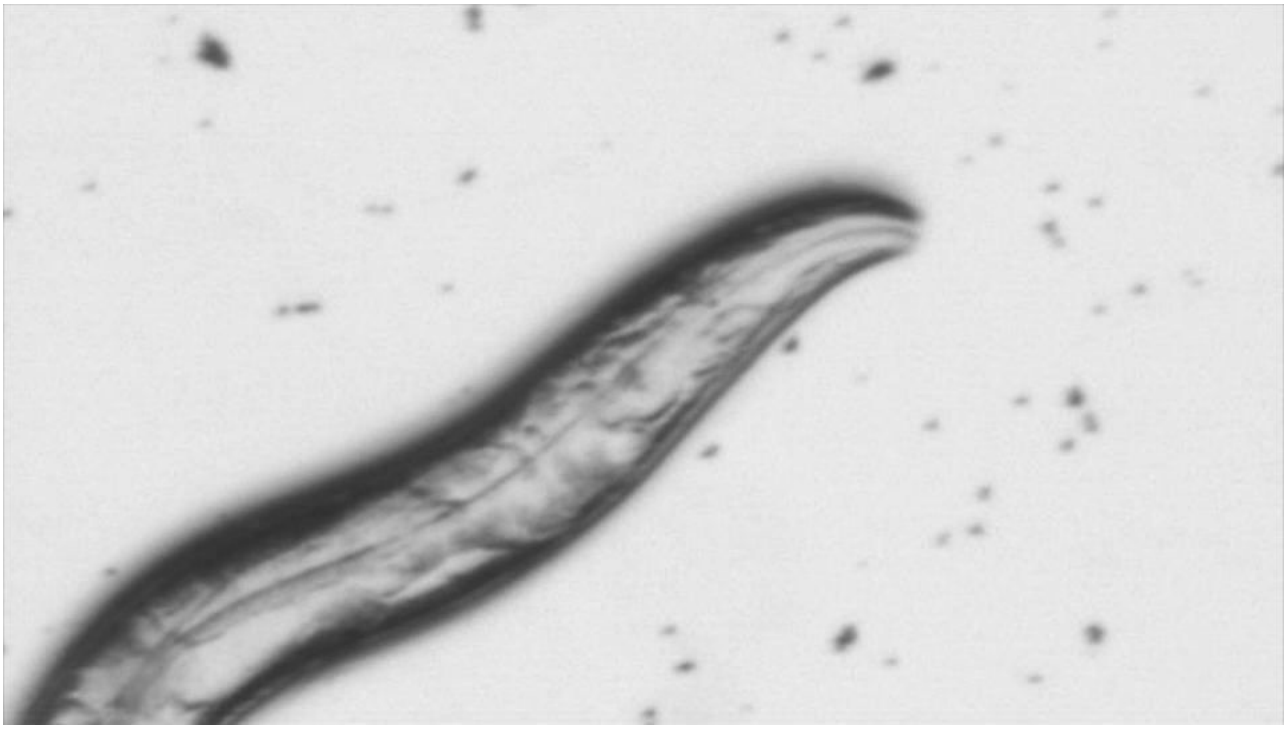

Movie 1. Recording of *C. elegans* worm eating Cu_2O particles through their muscular pharynx. The particles can be seen passing through the grinder and into the intestine. Recording is played back at half speed (30 frames per second) after being recorded at 60 frames per second.

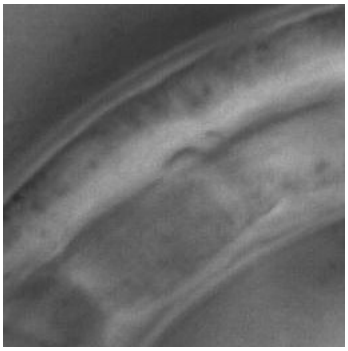

Movie 2. Ingested Cu_2O particles can be observed in the *C. elegans* intestine. Particle movement is induced by the defecation motor program which moves gut material between the anterior and posterior parts relative to the body. Recording is played back in real time (30 frames per second).

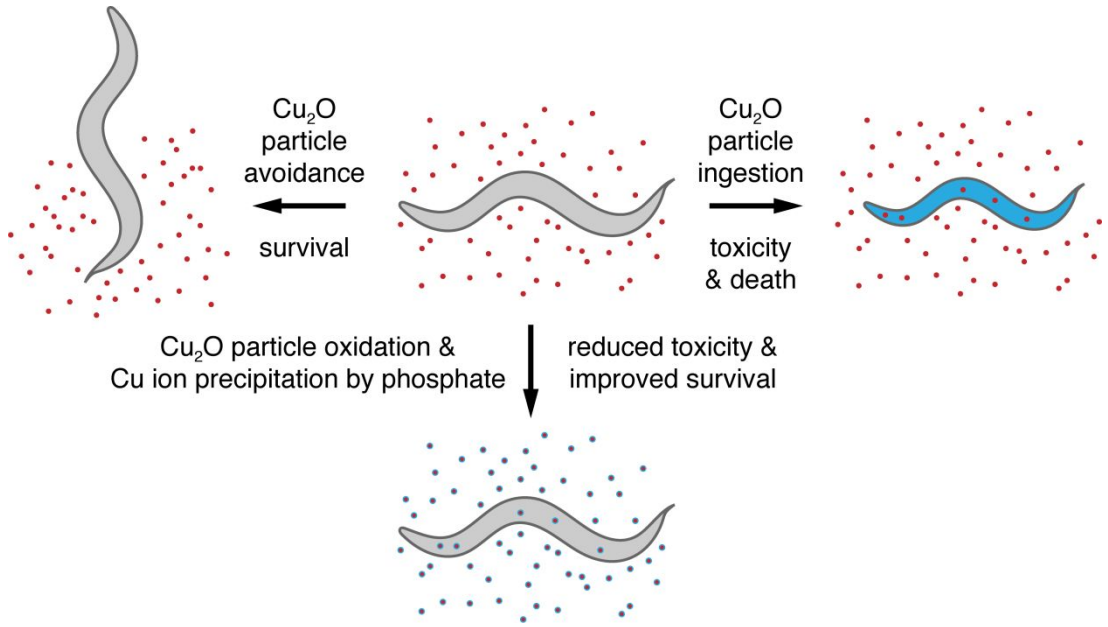

Graphical abstract. *C. elegans* worms (grey) encountering Cu_2O particles (red) can either avoid and survive (left) or they can ingest them (right) and experience toxic effects that resemble effects from Cu^{2+} uptake (blue). Phosphate induces Cu_2O particle oxidation (blue outlines) and Cu ion precipitation, allowing for improved survival even after ingestion (bottom).